Science of the Total Environment 1037 (2026) 181874

Contents lists available at ScienceDirect

Science of the Total Environment

journal homepage: www.elsevier.com/locate/scitotenv

Variations in the root-soil system influence the grapevine holobiont by shaping plant physiology and root microbiome

Massimo Guazzini [a,*], Ramona Marasco [b], Slobodanka Radović [c], Elisa Pellegrini [a], Marco Vuerich [a], Arianna Lodovici [a], Giorgia Dubsky De Wittenau [c], Eleonora Paparelli [c], Gabriele Magris [a,d], Laura Zanin [a], Marco Contin [a], Elisa De Luca [e], Daniele Daffonchio [b,f], Gabriele Di Gaspero [d], Fabio Marroni [a,*]

[a] Dipartimento di Scienze Agroalimentari, Ambientali e Animali (DI4A), Università di Udine, Udine, Italy
[b] Biological and Environmental Sciences and Engineering Division, King Abdullah University of Science and Technology (KAUST), Thuwal, Saudi Arabia
[c] IGA Technology Services, Udine, Italy
[d] Institute of Applied Genomics (IGA), Udine, Italy
[e] Vivai Cooperativi Rauscedo, Rauscedo, Italy
[f] Department of Agriculture Forestry and Food Sciences (DISAFA), University of Turin, Grugliasco, Turin, Italy

HIGHLIGHTS

- Soil composition drives grapevine holobiont structure and physiology.
- Multi-omics links soil traits to microbiome, leaf ions, and gene expression.
- Distinct soils modulate nutrient uptake and plant physiological responses.
- Root heat treatment leaves lasting transcriptomic imprints on roots.
- Soil autoclaving reshapes microbial communities with persistent effects.

GRAPHICAL ABSTRACT

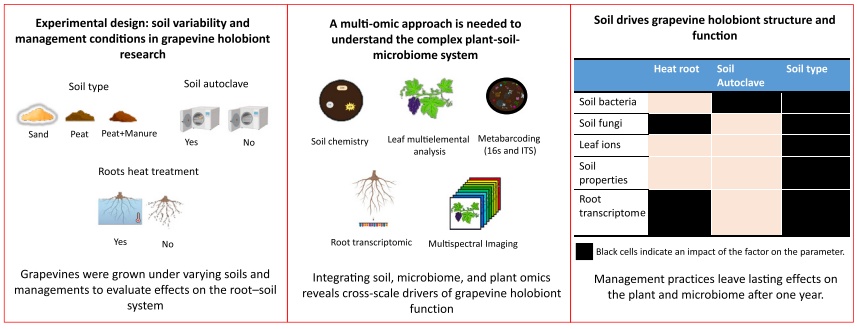

ARTICLE INFO

Keywords:
Grapevine
Holobiont
Soil microbiome
Plant-microbe interaction
Organic carbon
Data integration
Multi-omics

ABSTRACT

Soil-dwelling bacteria and fungi play a crucial role in plant health and productivity by engaging in complex interactions that shape and are shaped by soil physico-chemical properties. In this study, we employed a multi-omics approach to investigate how variations in soil composition affect the grapevine holobiont. Grape plantlets were grown in three distinct soil types, namely sand, peat, and peat-manure. To further assess how variation in soil and root conditions affects the holobiont's response, we included treatments involving soil autoclaving and root heat treatment across all soil types. We found that soil type significantly influences leaf multielement composition and concentration, while also shaping the bacterial and fungal communities associated with the plant rhizosphere. This shift led to changes in taxa involved in nitrogen fixation, biocontrol, and pathogenicity. Autoclaving soils consistently reduced bacterial diversity across all soil types, whereas fungal communities were less affected. In contrast, thermal treatment of roots had only a minor impact on microbial community

* Corresponding authors.
E-mail addresses: guazzini.massimo@spes.uniud.it (M. Guazzini), fabio.marroni@uniud.it (F. Marroni).

https://doi.org/10.1016/j.scitotenv.2026.181874
Received 12 November 2025; Received in revised form 20 April 2026; Accepted 10 May 2026
Available online 18 May 2026

composition but did induce transcriptional changes in the root and altered leaf macronutrient concentrations. Our findings indicate that differences in soil composition reshape the entire root-soil continuum, ultimately affecting plant physiology at multiple levels—from root function to leaf nutrient status. This highlights that the soil is not a passive growth medium but a key determinant of grape holobiont structure and function. These results reinforce the view that plant health and adaptation arise from integrated, dynamic interactions among the host, its associated microbiome, and the surrounding soil matrix.

1. Introduction

Soil bacteria and fungi establish close associations with plants and can significantly influence their health and productivity (Turner et al., 2013). This intimate relationship has led to the concept of the "plant holobiont", which refers to the integrated biological entity formed by the plant host and its associated microbiota, functioning as a single ecological unit (Vandenkoornhuyse et al., 2015).

The soil microbiome is primarily shaped by soil physico-chemical properties (Islam et al., 2020), which also directly affect plant physiology by regulating nutrient availability, water retention, and structural support (Lanyon et al., 2004). However, plants themself are key determinant in shaping their microbial associations, particularly in the rhizosphere—the narrow zone of soil surrounding plant roots—and adjacent soil still influenced by roots (Sánchez-Cañizares et al., 2017). Within this zone, plants actively recruit and select edaphic microorganisms through the release of root exudates and volatile organic compounds (Pascale et al., 2020). The composition of these exudates is also influenced by multiple environmental and climatic factors and varies among plant species and cultivars, thereby shaping the root microbiome and influencing plant-microbe interactions (Herz et al., 2018).

The interplay between plants and soil microbiota and its consequences for plant physiology, development, and resilience is an active and expanding field of research, particularly in grapevine (*Vitis vinifera*), a high-value crop cultivated worldwide (Sánchez-Cañizares et al., 2017). Grapevine is grown across a wide range of soil types that differ in physical and chemical properties, as well as in microbial load and composition (Marasco et al., 2013). Vines are typically propagated as rooted cuttings in nurseries, where they establish early symbiotic associations with *endo*- and *exo*-symbionts, which can result in either mutualistic or pathogenic relationships (Gramaje et al., 2022). To mitigate the risk of pathogenic associations, nurseries often apply treatments aimed at reducing disease incidence, such as root thermal treatment (Waite and May, 2005). However, these treatments can have a long-term impact on the structuring of the plant microbiome and physiology (Vukicevich et al., 2018). Once mature, plantlets are transplanted into vineyards where they encounter different environmental conditions and continue to develop complex and long-term interactions with the microorganisms living in the surrounding soil (Deloire et al., 2005; van Leeuwen, 2010).

The relationships between grapevine, soil, and their associated microbiomes are highly interconnected and interdependent. Numerous studies suggest that vineyard soil serves as the primary source of grapevine-associated microbiomes (Zarraonaindia et al., 2015). While previous studies have investigated how plant cultivars and soil types influence the composition of the grapevine microbiome (Rolli et al., 2017; Nerva et al., 2021; Marasco et al., 2022), these approaches often overlook the systemic feedbacks that define holobiont response, i.e., plant and microbiome. Recognizing this, we designed a multi-omics framework that simultaneously interrogates soil physico-chemical properties, microbial community structure (both bacterial and fungal), and grapevine physiological responses, including leaf elemental content, spectral emissions, and root transcriptomics. By evaluating the combined and individual effects of soil type and root thermal treatments, we sought to reveal how external environmental cues propagate through microbial assemblages and ultimately reshape plant molecular and physiological states. This unified approach enables us to assess the response of the grapevine holobiont and more accurately capture its adaptive behaviour as a whole.

2. Materials and methods

2.1. Experimental setup

One hundred cuttings of *Vitis vinifera* 'Trebbiano Romagnolo' clone R5 were grafted onto clonal rootstock Kober 5BB, rooted and grown under nursery conditions for one vegetative season at Vivai Cooperativi Rauscedo (Rauscedo, Italy), following standard practices of grapevine plant production. One-year-old cuttings were grown under open-field conditions at the experimental farm "Antonio Servadei" of the University of Udine from August 2021 (T0) until June 2022 (T1). Cuttings were planted in 2-litre potted soil using three commercially available growing substrates: (i) micronized river siliceous sand (Sabbia Fine Naturale, Axton; hereafter referred to as "sand"), (ii) mixture of sphagnum peat moss, green compost, and sand (Terriccio per Tappeti Erbosi, Geolia, Calvisano, Italy; hereafter referred to as "peat"), and (iii) sphagnum peat moss combined with bovine and equine manure (Terriccio con Stallatico, Geolia, Calvisano, Italy; hereafter referred to as "manure"). Half of the soil was subjected to a soil thermal treatment (i.e., autoclaved at 121 °C for 60 min) the day before planting. Half of the cuttings underwent root heat treatment, as follows. Heat treatment was applied by submerging roots in hot water at 50 °C for 45 min. The overall experimental design included 12 treatments: three soil types (3 levels: sand, peat, manure), root thermal treatment (2 levels: presence or absence), and soil thermal treatment (2 levels: presence or absence). Plants were irrigated using a drip irrigation system and allowed to grow for 11 months. NPK fertilizers were supplied on 01/06/2021 and 10/06/2021.

2.2. Sample collection

Bulk soil samples (in triplicate) were collected at planting (time 0, T0) and stored at −20 °C for further analyses. At the end of the experiment (time 1, T1), rhizosphere soil, root tissue, and leaves were collected from three potted plants per condition, as described below. An exception to this sampling plan was represented by the condition "sand autoclaved, root not treated", for which only one plant was available, and for the conditions "manure non-autoclaved, root not treated" and "peat non-autoclaved, root not treated," four samples were collected per condition. The complete list of samples is provided as Supplementary File S1. At T1, plants were uprooted, and soil was separated from the root ball using the pull and shake method to collect the rhizosphere and cleanse the roots for sampling (Duineveld et al., 1998). Rhizosphere samples were stored in 15 mL Falcon® tubes on dry ice until their transfer at −80 °C. The remaining soil was collected and stored at 4 °C for chemical analyses. Apical portions of non-lignified roots were also collected, snap frozen in liquid nitrogen and stored in dry ice until storage at −80 °C. For elemental analysis, the leaves were sliced using a ceramic knife, placed in 50 mL Falcon tubes, and stored in dry ice until storage at −20 °C.

2.3. Soil analysis

Bulk soil obtained at T0 and non-root-associated soil obtained at T1

were homogenized using a 2 mm sieve. Soil samples were divided into aliquots: about 500 g of soil was weighed into an aluminium tray and air-dried for subsequent physico-chemical analyses, and 200 g of fresh soil were stored in plastic bags at 4 °C for subsequent ATP (Adenosine Triphosphate) quantification. Soil pH was measured in soil-water suspension (1:2.5, weight-to-volume ratio) using a pH-meter (Crison, Italy). Electrical conductivity (EC) was measured in a 1:2 soil-to-water ratio (Rhoades, 1996) using an XS Cond 7 Vio conductivity meter (Giorgio Bormarc s.r.l., Italy) and reported as μS/cm. The analysis of Dissolved Organic Matter (DOM) included the determination of dissolved organic carbon (DOC) and dissolved total nitrogen (DN), measured as milligrams of dissolved element per gram of soil. An aliquot of 4 g of dry soil was mixed with 40 mL of Milli-Q® water and shaken overnight in the dark. After centrifugation and filtration, DOC and DN were measured using a TOC analyser (TOC-V_{CPN} Shimadzu, Kyoto). Total organic C and total N were measured on solid soil samples, after ball-mill grinding, with a CHNS elemental analyser (Vario Microcube, Elementar©). For organic C measurement, samples were previously treated with HCl to remove the inorganic C fraction. The C/N ratio was then calculated. The ATP extraction from fresh soil samples followed the acid-extraction method with modifications to account for ATP adsorption by soil colloids. Briefly, the extraction was carried out with trichloroacetic acid, orthophosphate, and imidazole solution (Redmile-Gordon et al., 2011) with 2 min of sonification on an ice bath. An ATP spike was added as an internal standard to estimate its extraction recovery. The measurement of ATP in soil extracts was carried out using an ATP kit based on bioluminescence reaction (BioThema luminescent assay, Sweden) at a "Spark" multimode microplate reader (Tecan Trading AG, Switzerland). ATP is reported as nanomoles of ATP per gram of soil. Collinearity between pairs of traits was defined as a Pearson $R^2 > 0.9$ at T0 and T1. In case of a collinear pair of traits, only one of the two was retained for analysis. The final physico-chemical parameters were DOC (Dissolved Organic Carbon), pH, ATP, and C/N.

2.4. Multispectral imaging of plants

At the end of the experiment, multispectral pictures of each plant were taken using two Micasense RedEdge-MX DUAL cameras. Images were captured by placing the potted plants on a flat surface against a neutral background, maintaining a consistent distance from the cameras. Before each image acquisition, a picture of the calibrated reflectance panel (CRP) was taken. CRP is a Lambertian surface with a reflectance calibration curve associated that allows for the conversion of raw pixel values into absolute reflectance. Moreover, to minimize the error during image capture due to changes in the light, a downwelling light sensor (DLS) has been coupled to the multispectral camera to adjust the readings to ambient light automatically. Since images captured at different wavelengths can have slight misalignments due to sensor differences and lens distortions, an image alignment step was performed before extracting reflectance values. This was done using the OpenCV 4.10.0.84 package in Python, applying an affine transformation to correct for shifts, rotations, and scale variations between images. The transformation was computed using key point detection and feature matching across the different wavelength bands, ensuring accurate pixel-to-pixel correspondence. The wavelength values for each plant were extracted using ImageJ 1.54 g software by selecting an area on a leaf surface perpendicular to the image captured, leaf by leaf, with at least 100 pixels and at least two leaves per plant, and using the R package "raster". This study focuses on NDVI (Normalized Difference Vegetation Index), CVI (Chlorophyll Vegetation Index), GDVI (Green Difference Vegetation Index), and NDWI (Normalized Difference Water Index). These indices use different waveband intensities to provide information on chlorophyll and water content, thus acting as proxies of plant physiology. Collinearity between pairs of traits was defined as a Pearson $R^2 > 0.9$. No collinearity was observed.

2.5. Multielemental analysis of leaves

The concentration (parts per million, ppm) of macro-nutrients, Ca (calcium), K (potassium), Mg (magnesium), P (phosphorus), S (sulphur), and micro-nutrients, Cu (copper), Fe (iron), Mn (manganese), Na (sodium), Zn (zinc) in grapevine leaves was determined by Inductively Coupled Plasma–Optical Emission Spectroscopy (ICP-OES 5800, Agilent Technologies, Santa Clara, USA). Leaves were oven-dried for 72 h at 50–60 °C and ground into powder. For each sample, around 100 mg of ground powder was digested with concentrated ultrapure HNO_3 using a microwave oven (ETHOS EASY, Milestone s.r.l., Sorisole, BG, Italy) according to the USEPA 3052 method "Plant Xpress" (Agency (USEPA), 1996). Element quantifications were carried out using certified multi-element standards. Collinearity between pairs of traits was defined as a Pearson $R^2 > 0.9$. No collinearity was observed.

2.6. Nucleic acid extraction, library preparation, and sequencing

DNA was extracted from rhizospheric soil from approximately 0.25 g of non-dried material stored at −80 °C using the DNeasy PowerLyzer PowerSoil kit from QIAGEN (Hilden, Germany), following the manufacturer's instructions. DNA was then sent to IGA Technology Services s.r.l. (Udine, Italy) for library preparation and sequencing. Libraries were prepared following the Illumina 16S Metagenomic Sequencing Library Preparation protocol in two amplification steps: an initial PCR amplification using locus-specific PCR primers and a subsequent amplification that integrates relevant flow-cell binding domains and unique indices (NexteraXT Index Kit, FC-131-1001/FC-131-1002). The locus-specific primers for the 16S rRNA gene were 341F (5′-CCTACGGGNGGCWGCAG-3′) and 805R (5′-GACTACHVGGGTATCTAATCC-3′). The locus-specific primers for the ITS rRNA were ITS3F (5′-GCATCGATGAAGAACGCAGC-3′) and ITS4R (5′-TCCTCCGCTTATTGATATGC-3′). Libraries were sequenced on NovaSeq 6000 instrument (Illumina, San Diego, CA) using a 250-bp paired-end mode.

For RNA sequencing, 100 mg of root samples were cleansed with tap water and ground in liquid nitrogen. Total RNA was extracted using the Spectrum Plant Total RNA Kit (SIGMA, The Netherlands). Libraries were prepared using the Universal Plus mRNA-Seq kit (Tecan Genomics, Redwood City, CA) following the manufacturer's instructions. Libraries were sequenced on a NovaSeq6000 instrument (Illumina, San Diego, CA) using a 150-bp paired-end sequencing mode. Raw transcriptomic reads were deposited in GEO under the accession GSE287854. Raw metabarcoding reads were deposited in the NCBI Sequence Read Archive under the accession PRJNA1217140.

2.7. Data analysis

Data analysis was performed using R version 4.4.2 where not differently specified. Adapters were removed using the *filterandtrim* function of DADA2 v1.34.0 (Callahan et al., 2016). Classification of 16S rRNA and ITS sequences was performed using DADA2 against the SILVA v138.1 (Quast et al., 2013) and UNITE v10.0 (Kõljalg et al., 2020) databases, respectively. Rarefaction curves were plotted using the *vegan* package v2.6.10 (Oksanen et al., 2024). Amplicon sequence variants (ASVs) not classified at the Kingdom level as "Bacteria" or "Fungi" were removed. Raw ASVs' counts were normalized by calculating their percentage relative to the total reads sequenced in each sample. ASVs with an average abundance lower than 0.001% were removed. Additional analyses were performed at the phylum and genus levels, aggregating ASVs based on their taxonomic classifications. The R (R Core Team, 2021) package *DESeq2* v1.46.0 (Love et al., 2014) was utilized to perform differential abundance analysis. For this step, the ASVs were merged, considering the lowest taxonomical level reached by the single ASV. Non-Metric Multidimensional Scaling (NMDS) analysis and alpha diversity analysis were conducted using the *vegan* package (Oksanen et al., 2024). The variable factors were represented as vectors on the

NMDS plot using the *envfit* function of the package *vegan*. Nested PERMANOVA analysis was performed using the *adonis* function of the package *vegan*. Functional prediction of bacterial species was performed using the FAPROTAX database and software v1.2.7 (Louca et al., 2016). Fungal genera were metabolically classified using FUNGuild (Version 1.1) and a manually curated version of the FUNGuild database (Nguyen et al., 2016). The list of FAPROTAX and FUNGuild functional categories considered in this study is visible in Supplementary Table S1.

RNA-seq reads were aligned using STAR software (Dobin et al., 2013) against the *Vitis vinifera* 12Xv0 genome assembly of the strain PN40024 (GCA_000003745.2) using the V2.1 version of gene model prediction. *DESeq2* (Love et al., 2014) was employed for differential gene expression analysis. To associate functions to gene models, the expression table was compared with the Phytozome database (Goodstein et al., 2012) file "Vvinifera_457_v2.1.annotation_info.txt," which includes the "Arabi_defline" column. This column provides the *Arabidopsis thaliana* gene description or annotation corresponding to the gene under analysis. GO annotation was performed by retrieving GO terms and their descriptors using the GO.db R package (Carlson, 2024) and the enrichR package (Kuleshov et al., 2016) for functional enrichment analysis. The genes mostly contributing to differentiation among variables were identified using the splsda function of the package mixOmics (Rohart et al., 2017) Classification of RNA viruses based on alignment of RNA sequences was performed using a previously described pipeline (Di Gaspero et al., 2022).

Data were plotted using the *pheatmap* (Kolde, 2019), *ggplot2* (Wilkinson, 2011), and *corrplot* (Wei and Simko, 2024) packages. Where not specified, the *cor.test* function from the *stats* package was used to perform Spearman correlation tests; *P*-values were adjusted for multiple testing using the false discovery rate (FDR) correction method.

Covariation among data sets was assessed using the RV.rtest function of the ade4 package (Dray and Dufour, 2007). The function block.splsda from the R package mixOmics (Rohart et al., 2017) was used to integrate the different data types and select the most important features from each data type. All scripts and R functions used in this study are available at https://github.com/genomeud/intevine.

3. Results

3.1. Physico-chemical parameters are affected by soil type and, to a lesser extent, by autoclaving

The physico-chemical parameters retained after collinearity analysis were DOC, pH, ATP and C/N (Supplementary Tables S2, S3). The four parameters showed significant differences across soil types, both at T0 and T1 (Supplementary Figs. S1 and S2, respectively). Such variations defined three different clusters in the ordination space of the NMDS plot at the two sampling points (Supplementary Fig. S3, Fig. 1a), with soil type explaining up to 89% and 86% of the variability, respectively, according to PERMANOVA analysis (Supplementary Tables S4, S5). A moderate effect of the soil autoclave treatment was observed both at T0 and T1; treatment of the root before transplantation did not affect the physico-chemical properties of the soil at T1.

3.2. Multispectral indices did not show variation across experimental conditions

Multispectral indices from collected leaves did not show a specific pattern of distribution in the NMDS ordination (Fig. 1B) as observed for soil physico-chemical analysis. However, soil type and the heat treatment of roots within soil-autoclave treatments significantly influenced the multispectral indices, explaining 27% and 23% of the variance, respectively, according to nested PERMANOVA analysis (Supplementary Table S6). Among the indices evaluated, only CVI and NDWI showed significant differences between soil types or heat root treatment (Supplementary Figs. S4 and S5), while none of the indices were affected by soil autoclaving.

3.3. Ion concentration in leaves is affect by soil type

NMDS analysis based on ion concentrations in the leaves separated sand samples from peat and manure (Fig. 1c). Nested PERMANOVA analysis showed that soil type was the only factor significantly contributing to this differentiation pattern (Supplementary Table S7). Such diversity is driven by seven of the analyzed elements that differed significantly in concentration across the three soil types (Supplementary Fig. S6).

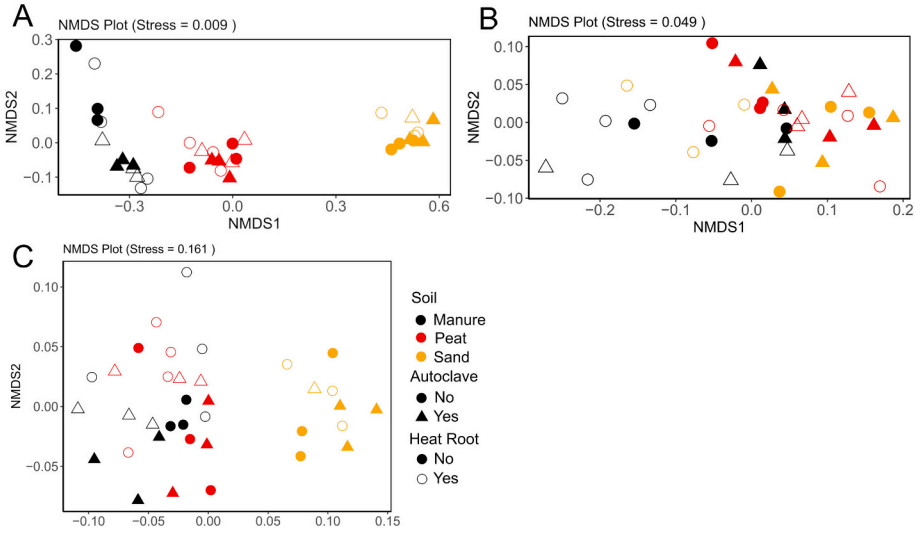

Fig. 1. Ordination of soil chemistry and leaf traits in grapevines after growth in different soils. Non-metric multidimensional scaling (NMDS) plot illustrating separation among (A) soil samples by chemical composition, (B) leaf samples by multispectral imaging indices, and (C) leaf samples by multielemental profiles at the end of the experiment (T1, 18 months).

3.4. Soil bacterial microbiome is affected by soil type and, to a lesser extent, by autoclaving

A total of 3,794,673 and 24,597,687 bacterial reads were retained for samples collected at T0 and T1, respectively (summary statistics in Supplementary Table S8), providing sufficient sequencing depth to ensure robust coverage of the bacterial community diversity (Supplementary Fig. S7A,B). At T0, diversity was shown only for the peat and manure samples, as the DNA recovered from the sand samples was not successfully amplified, likely due to the low abundance of microorganisms in this substrate before plant growth and irrigation. At the beginning of the experiment, peat soil showed a higher relative abundance of *Spirochaetota* and *Actinobacteriota* compared to manure soil, with *Gemmatimonadota* also being more abundant in peat soil (Supplementary Fig. S8A). *Bacillota* exhibited a higher relative abundance in autoclaved soil than in non-autoclaved soil, while *Proteobacteriota*, *Verrucomicrobiota*, and *Bacteroidota* were more abundant in non-autoclaved soil. NMDS analysis performed on bacterial ASVs showed that samples clustered by soil type and soil thermal treatment, defining significantly different groups according to PERMANOVA analysis (Supplementary Fig. S8B, Table S9). No significant differences in species richness and Shannon's index were observed (Supplementary Fig. S8D, E).

The differences in microbiome composition across soil types persisted in the rhizosphere and adjacent soil (i.e., root surrounding soil) at T1 (Fig. 2; PERMANOVA, Supplementary Table S10). While the most abundant phyla did not vary across soil (Fig. 2A), cluster analysis and NMDS revealed a separation of soils into three main clusters based on soil type; each cluster is further divided into two sub-clusters based on soil autoclaving (Fig. 2B,C, Supplementary Fig. S9). In addition, even if to a lesser extent, root thermal treatment influences the assembly of bacterial communities (Supplementary Fig. S9). Soil physico-chemical

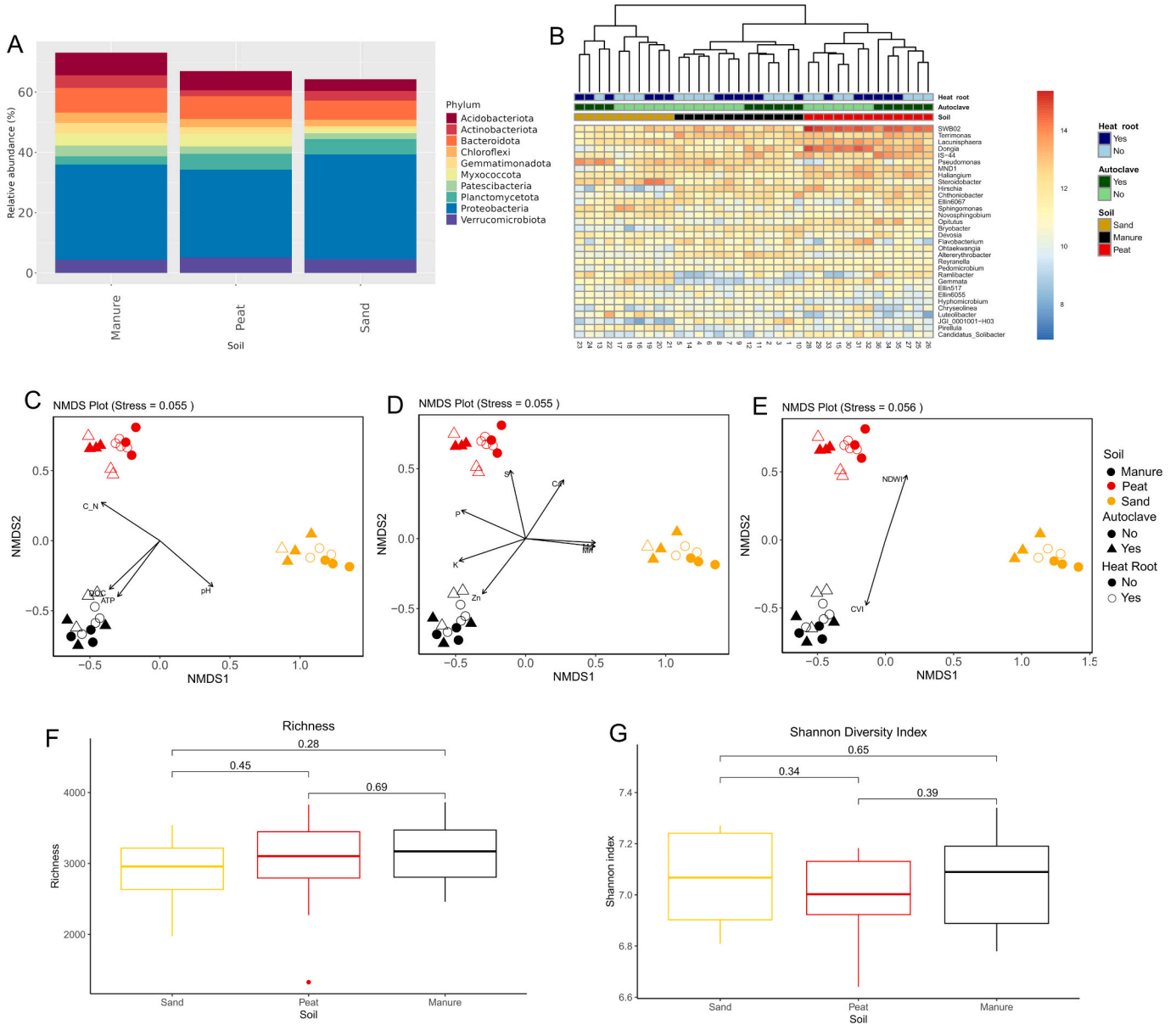

Fig. 2. Rhizosphere bacterial microbiome associated with grapevine after growth in different soils. (A) Average relative abundance of the most predominant phyla. (B) Heatmap of the most abundant genera with clustering analysis. NMDS analysis of the T1 bacterial rhizosphere microbiome, combined with (C) physico-chemical variables, (D) leaf multielemental concentrations, and (E) multispectral imaging indices, includes vectors representing only significant correlations identified by the envfit function. Boxplot with pairwise- Wilcoxon test (in brackets) of the (F) richness (i.e., observed number of ASVs; Kruskal-Wallis, $P = 0.5$) and (G) Shannon index (Kruskal-Wallis, $P = 0.51$) across the three types of soil.

parameters shown association with the bacterial communities. Fig. 2C shows NMDS of samples based on soil bacterial microbiome together with vectors of physico-chemical variables significantly affecting the NMDS ordination. C/N ratio was higher in peat, pH was higher in sand, and DOC and ATP were higher in manure.

Relationships were also found between the bacterial community and the multielemental analysis (Fig. 2D) between NMDS coordinates and nutrient concentration in leaves. Manure soil shows higher levels of potassium and zinc, peat shows higher level of sulphur and phosphorus, and sand shows higher levels of magnesium.

Fig. 2E shows the relationship between NMDS coordinates and multispectral imaging. Since from one of the sand samples (sample 13) it was not possible to extract the wavelength data, the NMDS was performed without it, hence the differences if compared with the previous. The manure soil cluster is associated with higher CVI and peat is associated with higher NDWI.

The three soil types did not show significant differences in alpha diversity measured as species richness and Shannon's diversity index (Fig. 2F,G). However, the composition of individual taxa showed several differences. A total of 542 bacterial genera exhibited differential abundance in at least one comparison, including soil type contrasts, soil autoclaving, or root heat treatments (Supplementary File S2). Seventeen bacterial genera showed different abundances across all soil types, both at T0 and T1. Among them are *Spirochaeta*, *Anaerolinea*, *Dongia*, and *Haliangium*. The effect of autoclaving soil resulted in 50 differential genera at T0 and 26 at T1. Only two of them, *Bacillus* and *Verrucosispora*, showed differences in both time points. Root thermal treatment had a minor effect on bacterial communities. Only three genera showed differences as a consequence of the treatment: *Caedibacter*, *Desulfuromonas*, and the I-8 genus of the family *Phycisphaeraceae*.

3.5. Soil fungal microbiome is affected by soil type and, to a lesser extent, by autoclaving

A total of 2,605,034 and 8,482,398 fungal reads were generated from ITS amplicons at T0 and T1, respectively. These reads were assigned to 600 and 774 fungal ASVs, respectively (Summary statistics are presented in Supplementary Table S8). Before planting (T0), peat samples were dominated by *Ascomycota,* and *Basidiomycota* abundance was negligible, while manure showed some contribution of *Basidiomycota* to the total fungal community (Supplementary Fig. S10A). NMDS, clustering and PERMANOVA analysis reveal the presence of two distinct clusters corresponding to the soil types, with the autoclave treatment further differentiating within each soil type (Supplementary Fig. S10B, C; Supplementary Table S11). Different soils showed different levels of fungal diversity; peat showed higher values of richness and Shannon's index than manure (Supplementary Fig. S10D,E). At T1, the soil retained a high relative abundance of *Ascomycota* and *Basidiomycota*. In addition, *Glomeromycota* were present at relatively high abundance, compared to what observed at T0 (Fig. 3A). Clustering analysis based on abundance of fungal genera showed some clustering based on soil type and some clusters determined by root heat treatment (Fig. 3B). NMDS analysis showed limited clustering across soil type and limited or no clustering across conditions (Fig. 3C–E), although PERMANOVA analysis indicated substantial contribution of all conditions to the variance (Supplementary Table S12). Higher DOC and ATP levels were associated with fungal communities in manure soil clusters, pH with those in sand, and C/N with peat ones (Fig. 3C). Increased levels of manganese, calcium, and magnesium were observed in the sand cluster, and a higher concentration of potassium in the manure cluster (Fig. 3D). Fungal communities showed significant correlations with the same multispectral indices as the bacterial population: the manure cluster was associated with higher CVI values and peat with higher NDWI values (Fig. 3E). When performing NMDS separately in each soil type, no major effect of soil thermal treatment or soil autoclaving was observed in each soil (Supplementary Fig. S11). However, several individual taxa showed different abundance across conditions and treatments. Specifically, a total of 84 fungal genera showed differences in at least one comparison between soil types (Supplementary File S3). Only the genus *Kernia* showed differences across all soil types, and only the genus *Chetomium* showed different abundance as a consequence of autoclaving soil at both time points. Ten genera showing differential abundance after thermal root treatment, namely *Qarounispora, Rhizoglomus, Septoglomus, Oliveonia, Glomus, Fusarium, Clonostachys, Amniculicola, Lophiostoma* and *Trichomonascus*. Richness and Shannon index were higher in peat, intermediate in sand and lower in manure soil (Fig. 3F,G).

3.6. Bacteria involved in nitrogen metabolism are more abundant in sand than in peat and amended peat

Functional prediction based on the taxonomic affiliation of bacterial and fungal clades allowed the identification of categories related to plant-association as mutualistic or pathogen functional traits (Supplementary Table S1). The distribution of such categories revealed that potential plant pathogens were less abundant in peat compared to other soils (Fig. 4A). Bacteria involved in processes related to the removal of nitrogen from the soil reservoir, such as nitrogen and nitrate respiration showed the higher relative abundance in sand and the lower in peat (Fig. 4B), while those able to perform nitrogen fixation were more abundant in sand and nearly absent in manure and peat (Fig. 4C). The potential fungal phytopathogens was significantly less abundant in the root surrounding soil of plants grown in manure soil compared to those from the other two types of soils (Fig. 5A). Fungi classified by FUNGUILD as arbuscular mycorrhizae did not show significant variation across soil types (Fig. 5B). Fungal parasites were more abundant in peat than in sand and manure (Fig. 5C). Finally, endophytic fungi (Fig. 5D) showed lower values in sand compared to peat, and no significant differences in other comparisons.

3.7. Gene expression is affected by soil type and, to a lesser extent, by root thermal treatment

On average, 21.8 million fragments per sample were properly mapped, ranging from 5.4 million to 48 million. Clustering analysis (Supplementary Fig. S12) and NMDS (Supplementary Fig. S13) did not show clear separation between soil types and conditions. PERMANOVA analysis shows that soil types, soil autoclaving, and root thermal treatment are significantly affecting the root transcriptome, although with a relatively small proportion of explained variance (Supplementary Table S13). Differential expression analysis identified 3489 differentially expressed genes (DEGs) when comparing expression in peat with expression in manure (peat vs. manure), 65 in sand vs. peat, and 5467 in sand vs. manure. Additionally, 1116 DEGs were identified in response to root heat treatment, while no DEGs were observed in response to autoclave treatment of soil substrates (Supplementary File S4). Genes differentially expressed in at least one soil comparison were enriched for GO categories related to photosynthetic activity, including chloroplast stroma and lipid metabolic activity (Fig. 6A). When assessing the effect of root thermal treatment, DEGs were enriched in terms related to translation processes and ribosome formation (Fig. 6B). The genes identified by discriminant analysis as contributing most to the discrimination between soil types or treatments are reported in Supplementary Table S14.

RNA-seq also enabled the detection of viral RNA; our results revealed the presence of four viruses, namely *Grapevine Pinot Gris Virus, Grapevine Rupestris Stem-pitting associated virus, Grapevine yellow-speckle viroid and hop stunt viroid*. Viral abundance was partly influenced by soil type, as evidenced by clustering analysis (Supplementary Fig. S14A). Supplementary Fig. S14B shows total viral abundance as a function of DOC, stratified by soil type and soil conditions. A positive correlation was observed between DOC and total viral abundance ($r = 0.3692$, $P = 8.491e{-}05$). In addition, Wilcoxon test showed that viral abundance

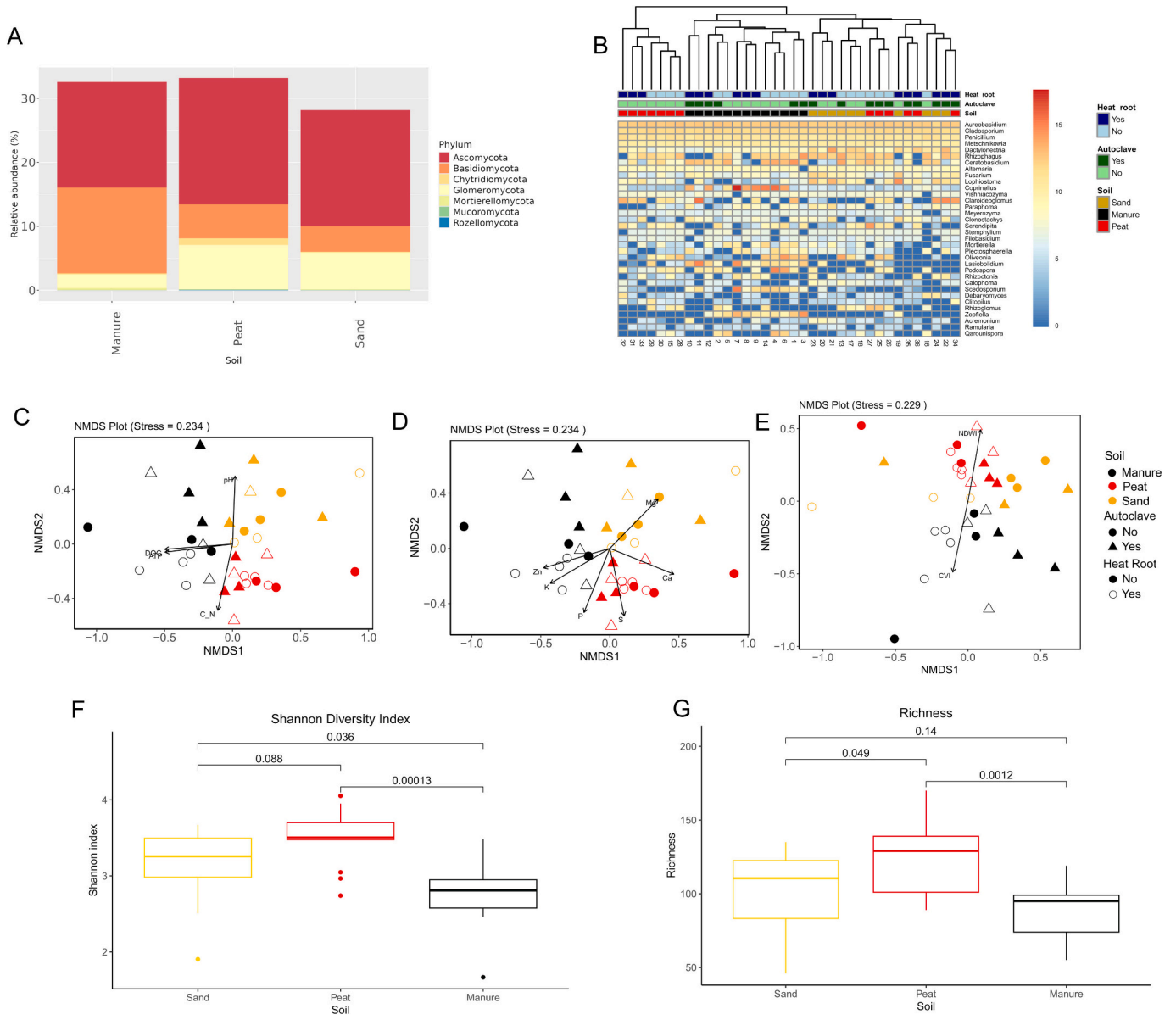

Fig. 3. Rhizosphere fungal microbiome associated with grapevine after growth in different soils. (A) Average relative abundance of the phyla identified. (B) Heatmap of the most abundant genera with clustering analysis. NMDS analysis of the T1 fungal rhizosphere microbiome, combined with (C) physico-chemical variables, (D) leaf multielemental concentrations, and (E) multispectral imaging indices, includes vectors representing only significant correlations identified by the envfit function, highlighting relationships between these parameters and bacterial distribution. Boxplot with pairwise- Wilcoxon test (in brackets) of the (F) richness (i.e., number of observed fungal ASVs; Kruskal-Wallis, $P = 0.00089$) and (G) Shannon index (Kruskal-Wallis, $P = 0.0029$) in the three types of soil.

was higher in manure (Supplementary Fig. S14C).

3.8. Integration of information

Analysis of the RV coefficient (Robert and Escoufier, 1976) was used as a multivariate analogue of correlation. Physico-chemical parameters showed significant correlation to all the other data types (Supplementary Fig. S15), while multispectral data showed correlation only with physico-chemical parameters.

Results of N-integration and feature selection for discriminating based soil types, autoclaving status and heat root treatment are listed in Supplementary Figs. S16, S17, and S18, respectively. Soil types were clearly clustered, similarly to what happened with individual data types. Several of the most contributing variables have been already identified analysing single data sets, such as pH, C/N ratio, and SWB02 (Supplementary Fig. S16). Differences in features between autoclaved and non-autoclaved soil allowed clustering based on treatment, with some misclassification (Supplementary Fig. S17), and clustering based on eat root treatment revealed more uncertainty in cluster determination compared to soil type and soil autoclaving (Supplementary Fig. S18).

4. Discussion

We present an integrative analysis of multi-omics framework to dissect how soil type and root thermal treatments shape the grapevine holobiont. By combining soil physico-chemical features, leaf ionomic measurements, multispectral imaging, root surrounding soil bacterial and fungal surveys, and root transcriptomics, we captured cross-scale linkages from edaphic inputs through microbial assembly to host physiology. In doing so, we showed that soil and its chemistry act as the master regulators: distinct soil types not only harboured unique bacterial and fungal communities but also imposed their signature on leaf

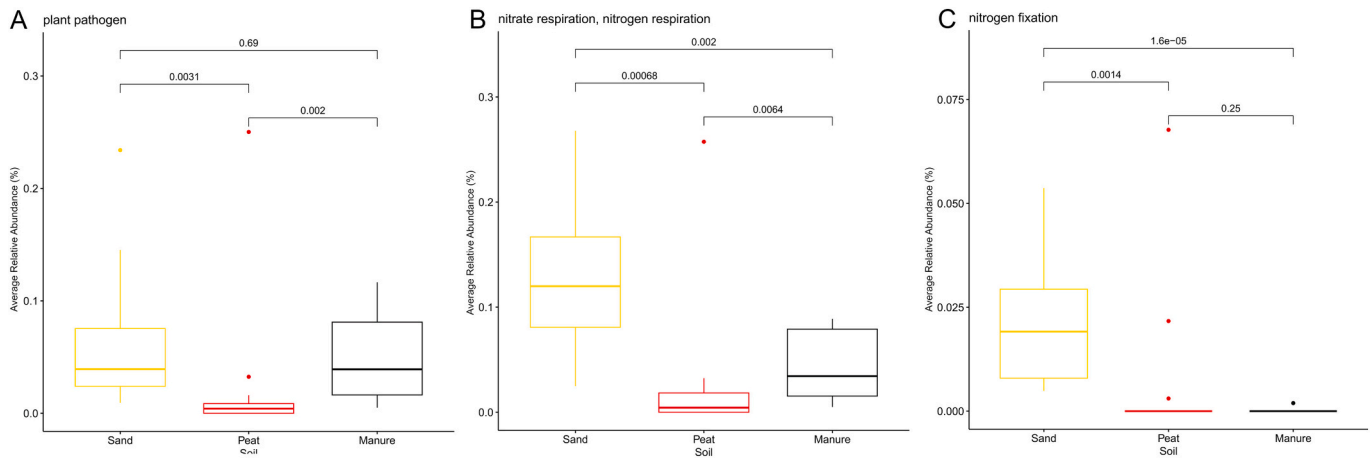

Fig. 4. Effect of soil in shaping predicted bacterial functional groups. Boxplot with pairwise- Wilcoxon test (in brackets) comparing the relative abundance of functional classes of bacterial species across the three types of soil at T1. Bacterial species related to (A) plant pathogens (Kruskal−Wallis, $P = 0.0016$), (B) nitrogen and nitrate respiration (Kruskal−Wallis, $P = 0.00014$), and (C) nitrogen fixation (Kruskal−Wallis, $P = 0.000015$).

nutrient profiles and spectral patterns, as well as shifts in root gene expression. Grapevine is cultivated worldwide across a wide range of soil types, from sandy to clay-rich and loamy soils (Deloire et al., 2005). Differences in soil properties influence water retention, nutrient availability, and root development, all of which affect grapevine performance and physiology (Quezada et al., 2014). Moreover, in line with the plant-soil-microbe feedback (Bettenfeld et al., 2022), soil properties also shape the composition and functional potential of edaphic microbiomes, including those associated with the rhizosphere and plants (Darriaut et al., 2022). A key factor is the type and amount of organic carbon present in the soil, which affects microbial activity and nutrient cycling (Hu et al., 2021). Soils rich in stable organic matter, such as humified carbon, tend to promote microbial diversity and activity, as well as healthier vines (Wang et al., 2025). Our data reinforced this paradigm and showed how bacterial community composition emerged as the most sensitive indicator of soil-driven grapevine holobiont differentiation when grown under different soils, even for a relative short time (11 months). Gene expression patterns were also influenced by soil type, particularly discriminating sand from peat and manure (Supplementary File S4). The concurrent enrichment of terms such as “chloroplast stroma” and “NAD binding” suggests that soil type may modulate the expression of genes involved in redox processes, potentially reflecting differences in the mineral composition between sand and the other substrates. In addition, genes associated with lipid metabolic processes varied between soil types, especially between sand and the more organic substrates (manure and peat). This pattern may reflect differences in carbon and nutrient availability, as well as microbial activity, which can influence lipid biosynthesis and remodelling in roots, particularly in relation to membrane dynamics and stress responses. The genes most contributing to differentiation between soils according to splsda also fit in this picture (Supplementary Table S14): VIT_215s0046g02500 is an adhesin-like, and may be involved in responses to different edaphic properties of soils or different microbial communities; VIT_200s0265g00070 is a ubiquitin-conjugating enzyme and may reflect broader regulatory adjustments in response to soil-dependent conditions.

Although soil type yielded the strongest influence, autoclaving can nonetheless leave a lasting imprint on the microbiome. Soil autoclaving is experimentally used for biotic clearing of soils, alters microbial composition, and is used to foster microbial recolonization (King et al., 2024). Autoclaving of soil for experiments in grapevine is sometimes performed in one cycle (Vukicevich et al., 2018) and sometimes with more than one cycles, separated by incubation time, to facilitate the elimination of spore-forming bacteria (King et al., 2024). Our approach was mild, using only one cycle. Nevertheless, this treatment disrupted microbial communities at the initial stage of the experiment. However, a recovery of community assemblages was observed 11 months post-treatment, suggesting high resilience or rapid recolonization. Such effect showed different levels between bacterial and fungal communities, where the former maintains a distinct trajectory, possibly due to higher sensitivity to initial treatment and/or a more defined niche colonization/selection and less heterogeneity across samples that allow the detection of a significant differentiation pattern.

Even if to a different extent, thermal root treatment mediates a shift in the fungal community assembly. Root thermal treatment is indeed a mainstay in grapevine nurseries to eliminate phylloxera, phytoplasmas, and other vascular pathogens from cuttings (Waite and May, 2005), however the collateral impacts on the native root-soil continuum associated microbiota that will be further established when grapevine cuttings are transplanted have rarely been examined. By stripping away resident symbionts and pathogens alike, root-heating treatments likely act as a strong ecological “reset” at the root–soil interface. Thermal shocks may create a temporal vacuum in which the first post-treatment colonizers can access exudates and attachment sites (Eichmeier et al., 2018), thus reshaping successional trajectories, with rapidly recolonizing species gaining priority. As expected, given that the new colonizers are drawn entirely from the bulk soil pool (here as sand, peat, and manure, autoclaved or not) (Zarraonaindia et al., 2015), it is plausible to expect that such treatment has a lower impact on the microbial community when different soils are compared. One could also expect that treated samples, facing recolonization, show higher differentiation than untreated samples, all originated from the same substrate with the same initial composition. However, our results suggest that the dispersion of samples treated with root heating is apparently not different from the dispersion of untreated samples (Fig. S11A, B, and C, filled symbols vs empty symbols).

Gene expression revealed that over a thousand root transcripts remained differentially expressed a season later. Functional analysis of differentially expressed genes revealed terms related to translation, ribosomes and mRNA binding, thus suggesting that the thermal treatment elicited long term reprogramming of processes related to transcription and translation. To further support this hypothesis, one of the genes mostly contributing to separation between treated and untreated roots is VIT_218s0001g13220 (Supplementary Table S14), a pentatricopeptide repeat that can bind RNA and affect gene expression (Miranda et al., 2017).

RNA-seq analysis also enables the detection of RNA viruses, which represent the main group of grapevine viral pathogens (Fuchs, 2020). In our dataset, we identified potential pathogens such as *Grapevine Pinot gris virus* and *Grapevine rupestris stem pitting-associated virus*, whose

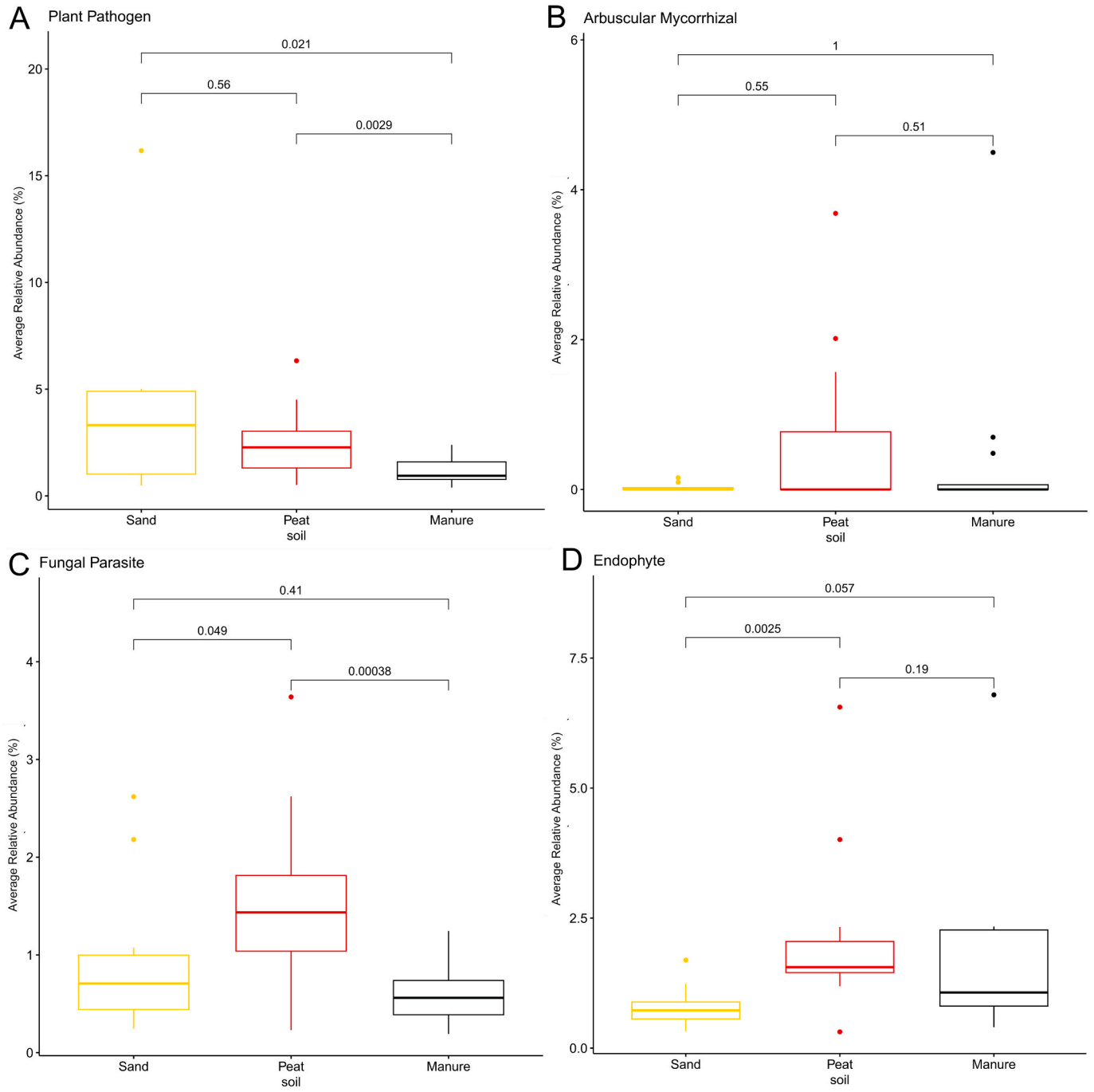

Fig. 5. Effect of soil in shaping predicted fungal functional guilds. Boxplot with pairwise-Wilcoxon test comparing the relative abundance of functional classes of fungal genera across the three types of soil at T1. Fungal genera classified as (A) plant pathogens (Kruskal–Wallis, $P = 0.0085$), (B) arbuscular mycorrhizal (Kruskal–Wallis, $P = 0.0031$), (C) fungal parasites (Kruskal–Wallis, $P = 0.0014$), and (D) endophyte mycorrhizal (Kruskal–Wallis, $P = 5e{-}04$).

abundance was higher in manure and positively correlated with DOC. These findings further highlight the complexity of the grapevine holobiont, where nutrient conditions that promote plant growth may simultaneously favor the proliferation of viral pathogens.

Differences between soil types were consistently captured by most data. In contrast, soil autoclaving and heat root treatment left more modest signatures in the measured data sources. However, the integration of different data types allowed improving discrimination between treated and untreated samples.

While our experimental design focused solely on the effect of different soil types, nursery substrates are often reused for the cultivation of other plants. This aspect was not explicitly tested in this study; however, the previous cultivation history of a substrate is likely to influence both its biotic and abiotic properties. The soils used in this experiment are broadly comparable to substrates used in grapevine nursery systems; however, pure sand is typically not used alone, but rather incorporated into sand-rich soils. This suggests that similar outcomes may be expected under nursery production conditions. In contrast, extrapolation to vineyard conditions is less straightforward due to differences in plant physiology and management practices (e.g., root heat treatments are not feasible for mature plants). Our results underscore the importance of considering the plasticity of soil microbiomes and the potential of targeted soil treatments to shape soil–microbe–plant interactions in favor of plant-soil-microbe positive feedback, i.e.,

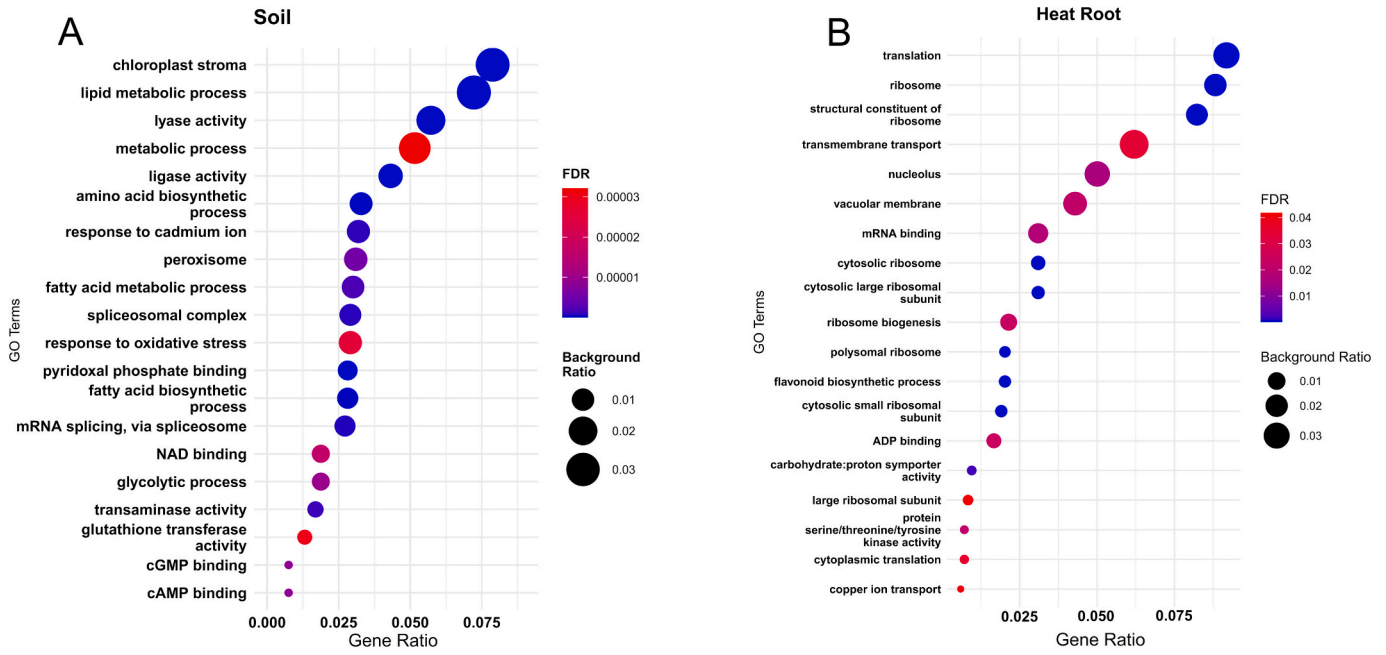

Fig. 6. Differential gene expression in grapevine root tissues under different conditions. Gene ontology (GO) enrichment dot plot illustrating functional enrichment analysis. Gene ratio represents the proportion of genes associated with each GO term, background ratio indicates the proportion of genes in the reference set, and False Discovery Rate (FDR) reflects statistical significance. (A) Top 20 GO categories differentially enriched in at least one soil comparison. (B) All differentially enriched GO categories in the heat root treatment.

enrichment of mutualistic interactions. Such knowledge can inform more sustainable and effective soil management strategies, both in grapevine nurseries and in vineyard management, ultimately supporting vine propagation and plant productivity.

CRediT authorship contribution statement

Massimo Guazzini: Writing – review & editing, Writing – original draft, Software, Investigation, Data curation. **Ramona Marasco:** Writing – review & editing, Supervision, Resources, Investigation. **Slobodanka Radović:** Writing – review & editing, Resources, Investigation. **Elisa Pellegrini:** Writing – review & editing, Resources, Investigation. **Marco Vuerich:** Resources, Investigation. **Arianna Lodovici:** Writing – review & editing, Investigation. **Giorgia Dubsky De Wittenau:** Investigation. **Eleonora Paparelli:** Investigation. **Gabriele Magris:** Investigation. **Laura Zanin:** Resources, Investigation. **Marco Contin:** Writing – review & editing, Resources, Investigation. **Elisa De Luca:** Writing – review & editing, Resources. **Daniele Daffonchio:** Writing – review & editing, Supervision, Resources. **Gabriele Di Gaspero:** Writing – review & editing, Resources, Investigation, Conceptualization. **Fabio Marroni:** Writing – review & editing, Supervision, Software, Resources, Investigation, Conceptualization.

Funding information

This work was supported by the Departmental Strategic Plan (PSD) of the University of Udine - Interdepartmental Project on Artificial Intelligence (2020–25) to Prof. Laura Zanin and Prof. Fabio Marroni, and by King Abdullah University of Science and Technology (KAUST) through the baseline research funds to Prof. Daniele Daffonchio.

Declaration of competing interest

The authors declare that they have no known competing financial interests or personal relationships that could have appeared to influence the work reported in this paper.

Acknowledgements

Authors gratefully acknowledge the help of Nicoletta Felice from the University of Udine for DNA and RNA extraction. Authors gratefully acknowledge the help of Romina Carpi from Azienda Sperimentale A. Servadei, for technical help in plant cultivation. We thank IGA technology services s.r.l. for support in sequencing experiments. We also thank Laura D'Andrea for her assistance with DNA extraction and soil chemistry analysis. The authors also wish to thank the VSRP Internship Program of King Abdullah University of Science and Technology (KAUST) for supporting this research.

Appendix A. Supplementary data

Supplementary data to this article can be found online at https://doi.org/10.1016/j.scitotenv.2026.181874.

Data availability

Raw RNA-seq reads were deposited in GEO under the accession GSE287854. Raw metabarcoding reads were deposited in the NCBI Sequence Read Archive under the accession PRJNA1217140. Scripts and functions used for analysis are available at https://github.com/genomeud/intevine.

References

Agency (USEPA), U.S.E.P, 1996. EPA Method 3052: microwave assisted acid digestion of siliceous and organically based matrices. Available at:, U.S. Environmental Protection Agency. https://www.epa.gov.

Bettenfeld, P., et al., 2022. The microbiota of the grapevine holobiont: a key component of plant health. J. Adv. Res. 40, 1–15. Available at: https://doi.org/10.1016/j.jare.2021.12.008.

Callahan, B.J., et al., 2016. DADA2: high-resolution sample inference from Illumina amplicon data. Nat. Methods 13 (7), 581–583. Available at: https://doi.org/10.1038/nmeth.3869.

Carlson, M., 2024. GO.db: a set of annotation maps describing the entire Gene Ontology. Available at https://bioconductor.org/packages//release/data/annotation/html/GO.db.html.

Darriaut, R., et al., 2022. Soil composition and rootstock genotype drive the root associated microbial communities in young grapevines. Front. Microbiol. 13. https://doi.org/10.3389/fmicb.2022.1031064 (Available at:).
Deloire, A., et al., 2005. Grapevine responses to terroir: a global approach. J. Int. Sci. Vigne Vin 39, 149–162 (Available at:) 10.20870/oeno-one.2005.39.4.888.
Di Gaspero, G., et al., 2022. Evaluation of sensitivity and specificity in RNA-Seq-based detection of grapevine viral pathogens. J. Virol. Methods 300, 114383 (Available at:) https://doi.org/10.1016/j.jviromet.2021.114383.
Dobin, A., et al., 2013. STAR: ultrafast universal RNA-seq aligner. Bioinf. (Oxf.) 29 (1), 15–21 (Available at:) https://doi.org/10.1093/bioinformatics/bts635.
Dray, S., Dufour, A.-B., 2007. The ade4 package: implementing the duality diagram for ecologists. J. Stat. Softw. 22, 1–20 (Available at:) 10.18637/jss.v022.i04.
Duineveld, B.M., et al., 1998. Analysis of the dynamics of bacterial communities in the rhizosphere of the chrysanthemum via denaturing gradient gel electrophoresis and substrate utilization patterns. Appl. Environ. Microbiol. 64 (12), 4950–4957. Available at: https://doi.org/10.1128/AEM.64.12.4950-4957.1998.
Eichmeier, A., et al., 2018. High-throughput amplicon sequencing-based analysis of active fungal communities inhabiting grapevine after hot-water treatments reveals unexpectedly high fungal diversity. Fungal Ecol. 36, 26–38 (Available at:) https://doi.org/10.1016/j.funeco.2018.07.011.
Fuchs, M., 2020. Grapevine viruses: a multitude of diverse species with simple but overall poorly adopted management solutions in the vineyard. J. Plant Pathol. 102 (3), 643–653 (Available at:) https://doi.org/10.1007/s42161-020-00579-2.
Goodstein, D.M., et al., 2012. Phytozome: a comparative platform for green plant genomics. Nucleic Acids Res. 40 (D1), D1178–D1186 (Available at:) https://doi.org/10.1093/nar/gkr944.
Gramaje, D., et al., 2022. Exploring the temporal dynamics of the fungal microbiome in rootstocks, the lesser-known half of the grapevine crop. J. Fungi 8 (5), 421 (Available at:) https://doi.org/10.3390/jof8050421.
Herz, K., et al., 2018. Linking root exudates to functional plant traits. PloS One 13 (10), e0204128. Available at: https://doi.org/10.1371/journal.pone.0204128.
Hu, H., et al., 2021. Significant association between soil dissolved organic matter and soil microbial communities following vegetation restoration in the Loess Plateau. Ecol. Eng. 169, 106305 (Available at:) https://doi.org/10.1016/j.ecoleng.2021.106305.
Islam, W., et al., 2020. Role of environmental factors in shaping the soil microbiome. Environ. Sci. Pollut. Res. 27 (33), 41225–41247 (Available at:) https://doi.org/10.1007/s11356-020-10471-2.
King, W.L., et al., 2024. Autoclaving is at least as effective as gamma irradiation for biotic clearing and intentional microbial recolonization of soil. mSphere 9 (7), e00476-24 (Available at:) https://doi.org/10.1128/msphere.00476-24.
Kolde, R., 2019. Pheatmap: Pretty Heatmaps (R package version), 1(2), p. 726.
Kõljalg, U., et al., 2020. The taxon hypothesis paradigm—on the unambiguous detection and communication of taxa. Microorganisms 8 (12), 1910 (Available at:).
Kuleshov, M.V., et al., 2016. Enrichr: a comprehensive gene set enrichment analysis web server 2016 update. Nucleic Acids Res. 44 (Web Server issue), W90–W97 (Available at:) https://doi.org/10.1093/nar/gkw377.
Lanyon, D., Cass, A., Hansen, D., 2004. The effect of soil properties on vine performance. In: CSIRO Land and Water Technical Report. https://doi.org/10.4225/08/586be7e218029 (34/04. Available at:).
Louca, S., Parfrey, L.W., Doebeli, M., 2016. Decoupling function and taxonomy in the global ocean microbiome. Science 353 (6305), 1272–1277 (Available at:) https://doi.org/10.1126/science.aaf4507.
Love, M.I., Huber, W., Anders, S., 2014. Moderated estimation of fold change and dispersion for RNA-seq data with DESeq2. Genome Biol. 15 (12), 550 (Available at:) https://doi.org/10.1186/s13059-014-0550-8.
Marasco, R., et al., 2013. Plant growth promotion potential is equally represented in diverse grapevine root-associated bacterial communities from different biopedoclimatic environments. BioMed. Res. Int. 2013, 491091 (Available at:) https://doi.org/10.1155/2013/491091.
Marasco, R., et al., 2022. Rootstock–scion combination contributes to shape diversity and composition of microbial communities associated with grapevine root system. Environ. Microbiol. 24 (8), 3791–3808 (Available at:) https://doi.org/10.1111/1462-2920.16042.
Miranda, R.G., et al., 2017. RNA-binding specificity landscape of the pentatricopeptide repeat protein PPR10. RNA 23 (4), 586–599 (Available at:) https://doi.org/10.1261/rna.059568.116.
Nerva, L., et al., 2021. Microscale analysis of soil characteristics and microbiomes reveals potential impacts on plants and fruit: vineyard as a model case study. Plant Soil 462 (1), 525–541 (Available at:) https://doi.org/10.1007/s11104-021-04884-2.
Nguyen, N.H., et al., 2016. FUNGuild: an open annotation tool for parsing fungal community datasets by ecological guild. Fungal Ecol. 20, 241–248 (Available at:) https://doi.org/10.1016/j.funeco.2015.06.006.
Oksanen, J., et al., 2024. vegan: community ecology package. https://cran.r-project.org/web/packages/vegan/index.html (Available at:; Accessed: July 25, 2024).
Pascale, A., et al., 2020. Modulation of the root microbiome by plant molecules: the basis for targeted disease suppression and plant growth promotion. Front. Plant Sci. 10, 1741 (Available at:) https://doi.org/10.3389/fpls.2019.01741.
Quast, C., et al., 2013. The SILVA ribosomal RNA gene database project: improved data processing and web-based tools. Nucleic Acids Res. 41 (D1), D590–D596 (Available at:) https://doi.org/10.1093/nar/gks1219.
Quezada, C., et al., 2014. Influence of soil physical properties on grapevine yield and maturity components in an Ultic Palexeralf soils, central-southern, Chile. Open. J. Soil. Sci. 4 (4), 127–135 (Available at:) https://doi.org/10.4236/ojss.2014.44016.
R Core Team, 2021. R: A Language and Environment for Statistical Computing. R Foundation for Statistical Computing, Vienna, Austria (Available at: https://www.R-project.org/).
Redmile-Gordon, M., White, R.P., Brookes, P.C., 2011. Evaluation of substitutes for paraquat in soil microbial ATP determinations using the trichloroacetic acid based reagent of Jenkinson and Oades (1979). Soil Biol. Biochem. 43 (5), 1098–1100. Available at: https://doi.org/10.1016/j.soilbio.2011.01.007.
Rhoades, J.D., 1996. Salinity: electrical conductivity and total dissolved solids. In: Methods of Soil Analysis. John Wiley & Sons, Ltd, pp. 417–435 (Available at:) https://doi.org/10.2136/sssabookser5.3.c14.
Robert, P., Escoufier, Y., 1976. A unifying tool for linear multivariate statistical methods: the RV- coefficient. J. R. Stat. Soc. Ser. C. Appl. Stat. 25 (3), 257–265 (Available at:) https://doi.org/10.2307/2347233.
Rohart, F., et al., 2017. mixOmics: an R package for 'omics feature selection and multiple data integration. PLoS Comput. Biol. 13 (11), e1005752 (Available at:) https://doi.org/10.1371/journal.pcbi.1005752.
Rolli, E., et al., 2017. Root-associated bacteria promote grapevine growth: from the laboratory to the field. Plant Soil 410 (1), 369–382 (Available at:) https://doi.org/10.1007/s11104-016-3019-6.
Sánchez-Cañizares, C., et al., 2017. Understanding the holobiont: the interdependence of plants and their microbiome. Curr. Opin. Microbiol. 38, 188–196 (Available at:) https://doi.org/10.1016/j.mib.2017.07.001.
Turner, T.R., James, E.K., Poole, P.S., 2013. The plant microbiome. Genome Biol. 14 (6), 209 (Available at:) https://doi.org/10.1186/gb-2013-14-6-209.
van Leeuwen, C., 2010. 9 - terroir: the effect of the physical environment on vine growth, grape ripening and wine sensory attributes. In: Reynolds, A.G. (Ed.), Managing Wine Quality, Woodhead Publishing Series in Food Science, Technology and Nutrition. Woodhead Publishing, pp. 273–315. https://doi.org/10.1533/9781845699284.3.273.
Vandenkoornhuyse, P., et al., 2015. The importance of the microbiome of the plant holobiont. New Phytol. 206 (4), 1196–1206 (Available at:) https://doi.org/10.1111/nph.13312.
Vukicevich, E., et al., 2018. Groundcover management changes grapevine root fungal communities and plant-soil feedback. Plant Soil 424 (1), 419–433 (Available at:) https://doi.org/10.1007/s11104-017-3532-2.
Waite, H., May, P., 2005. The effects of hot water treatment, hydration and order of nursery operations on cuttings of Vitis vinifera cultivars. Phytopathol. Mediterr. 44 (2), 144–152 (Available at: https://www.jstor.org/stable/26463197).
Wang, W., et al., 2025. Soil organic matter composition affects ecosystem multifunctionality by mediating the composition of microbial communities in long-term restored meadows. Environ. Microbiomes 20 (1), 22 (Available at:) https://doi.org/10.1186/s40793-025-00678-6.
Wei, T., Simko, V., 2024. R package 'corrplot': visualization of a correlation matrix (version 0.95). Available at https://github.com/taiyun/corrplot.
Wilkinson, L., 2011. ggplot2: elegant graphics for data analysis by WICKHAM, H. Biometrics 67 (2), 678–679 (Available at:) https://doi.org/10.1111/j.1541-0420.2011.01616.x.
Zarraonaindia, I., et al., 2015. The soil microbiome influences grapevine-associated microbiota. mBio 6 (2), e02527-14 (Available at:) https://doi.org/10.1128/mBio.02527-14.